Journal of Zhejiang University SCIENCE A
ISSN 1673-565X (Print); ISSN 1862-1775 (Online)
www.zju.edu.cn/jzus; www.springerlink.com
E-mail: jzus@zju.edu.cn

Wind-induced response analysis of a wind turbine tower including the blade-tower coupling effect*

Xiao-bo CHEN[1], Jing LI[1], Jian-yun CHEN[†‡1,2]

([1]*School of Civil and Hydraulic Engineering, Dalian University of Technology, Dalian 116024, China*)

([2]*State Key Laboratory of Coastal and Offshore Engineering, Dalian University of Technology, Dalian 116024, China*)

[†]E-mail: eerd001@dlut.edu.cn

Received Oct. 28, 2008; Revision accepted Jan. 5, 2009; Crosschecked Sept. 10, 2009

Abstract: To analyze wind-induced response characteristics of a wind turbine tower more accurately, the blade-tower coupling effect was investigated. The mean wind velocity of the rotating blades and tower was simulated according to wind shear effects, and the fluctuating wind velocity time series of the wind turbine were simulated by a harmony superposition method. A dynamic finite element method (FEM) was used to calculate the wind-induced response of the blades and tower. Wind-induced responses of the tower were calculated in two cases (one included the blade-tower coupling effect, and the other only added the mass of blades and the hub at the top of the tower), and then the maximal displacements at the top of the tower of the tow cases were compared with each other. As a result of the influence of the blade-tower coupling effect and the total base shear of the blades, the maximal displacement of the first case increased nearly by 300% compared to the second case. To obtain more precise analysis, the blade-tower coupling effect and the total base shear of the blades should be considered simultaneously in the design of wind turbine towers.

Key words: Fluctuating wind velocity, Mean wind velocity, Tower, Blade, Coupling, Wind shear effect, Vibration
doi:10.1631/jzus.A0820750 **Document code:** A **CLC number:** TU311.3; TK8

INTRODUCTION

Wind-induced response analyses have attracted intensive attention in the structural design process of wind turbines. Owing to its large slenderness ratio and significant flexibility, a wind turbine can be regarded as a flexibly dynamic multi-body system (Jin *et al*., 2008; Lanzafame and Messina, 2007; Chattot, 2007), and its components have coupling effects during the vibration which will change the wind-induced response of towers (Jelenic and Crisfield, 2001). Blades and a tower are main structural components of a wind turbine. Usually, the blades with a complex aerodynamic outline are made of glass reinforced plastic (GRP), and the tower is composed by a steel tower or steel tube truss. Operating characteristics of a wind turbine are determined directly by the dynamic characteristics of the tower and blades (Lesaffre *et al*., 2007). The wind-induced responses of blades and towers were studied by many scholars. Naguleswaran (1994) simplified rotating blades to cantilever beam to analyze their dynamic characteristics, and this method was used in many research fields. Lee *et al*.(2001) carried out experimental studies on the vibration characteristics of rotating blades. With the combination of finite element method (FEM) and practical running characteristics, Baumgart (2002) analyzed the dynamic response of blades under the wind loads, but the analysis process was complex. Lavassas *et al*.(2003) used 5028 four-node shell elements to analyze the dynamic response of a tower, and the results showed that analytical precision was closely related to mesh density.

---

‡ Corresponding author

* Project supported by the National Natural Science Foundation of China (No. 50708015), and the Program for New Century Excellent Talents in University (No. NCET-06-0270), China

Some studies about the blade-tower coupling effect were carried out by Murtagh *et al*.(2005). They used the mode acceleration method to examine the along wind-induced response of the blades and tower. All the works above laid a foundation for studying the dynamic response of wind turbines.

Winds are made of fluctuating wind and mean wind components. According to the wind-shear effect, the mean component can be calculated by the height of calculation point and roughness length, and the fluctuating component can be numerically simulated by the fluctuating wind power spectrum (Kareem, 2008; Kubota *et al*., 2008; Di Paola and Zingales, 2008; Schindler, 2008). The harmony superposition method was adopted by Deodatis (1996) to simulate the ergodic random wind field, and the fluctuating wind velocity of high-rise buildings was simulated by the Kaimal spectrum. To simulate the multivariable uniform Gaussian random process, general simulation theories of the stationary random fields were proposed (Shinozuka, 1971; Shinozuka and Jan, 1972). Yang (1972) successfully deployed fast Fourier transform (FFT) to simulate the wind velocity simulation, and the computational efficiency was improved. Di Paola (1998) presented a power spectrum decomposition method by eigenvalue, and also discussed the physical meanings of eigenvalue and orthogonal eigenvector. Yang *et al*.(1997) used explicit forms to express the Cholesky decomposition of the fluctuating wind power spectrum of the bridge, and then improved the simulation precision.

The above studies present some general theories of the wind velocity simulation, but these theories need further research for their application in the wind velocity simulation. At present, few related analyses are available regarding the wind velocity simulation of the rotating blades. For the rotating blade, the height (relative to the hub) of each calculation point on the blade varies continuously during the rotation, so the mean wind velocity of each calculation point will alter with the height according to the wind-shear effect. Besides, the fluctuating wind velocity of each point on the swept area is also different, thus a specific simulation method is needed to simulate the wind velocity of the rotating blade. Based on the above characteristics, the tower and the swept area of a blade were divided into a finite number of calculation points by the outline characteristics of a wind turbine, and then the fluctuating wind velocity and the mean wind velocity of these discrete points can be obtained. An approximate combination method of the fluctuating wind velocity and the mean wind velocity was introduced in detail, laying a foundation for simulating the wind velocity of a rotating blade factually and effectively.

VIRBRATION EQUATION OF TOWERS INCLUDING THE BLADE-TOWER COUPLING EFFECT

To analyze the blade-tower coupling vibration characteristics, a blade can be simplified to the variable cross-section rectangular cantilever beam as the complex aerodynamic outline. In the dynamic calculation process, the blades and the tower are both equivalent to the multi-degree of a freedom system. The vibration equation of the blades under the wind loads can be obtained by the D'Alembert principle (Clough and Penzien, 1975):

$$\boldsymbol{M}_{\mathrm{B}}\ddot{\boldsymbol{v}}+\boldsymbol{C}_{\mathrm{B}}\dot{\boldsymbol{v}}+\boldsymbol{K}_{\mathrm{B}}\boldsymbol{v}=\boldsymbol{F}_{\mathrm{B}}(t), \tag{1}$$

where $\boldsymbol{M}_{\mathrm{B}}$ is the mass matrix of blades, $\boldsymbol{C}_{\mathrm{B}}$ the damping matrix of blades, $\boldsymbol{K}_{\mathrm{B}}$ the stiffness matrix of blades, $\ddot{\boldsymbol{v}}$ the acceleration coordinates of blades, $\dot{\boldsymbol{v}}$ the velocity coordinates of blades, $\boldsymbol{v}$ the displacement coordinates of blades, and $\boldsymbol{F}_{\mathrm{B}}(t)$ the wind force on the blades which can be calculated by Eq.(2).

Two wind components both generate a force on the structure, and the force is related to the density of air, the effective action area of wind loads, etc. Thus, the wind load can be expressed as

$$F(t)=\frac{1}{2}C_{\mathrm{D}}\rho_{\mathrm{air}}A(\overline{w}+w')^2, \tag{2}$$

where C_{D} is the drag coefficient, ρ_{air} the density of air, A the effective action area of wind load, $\overline{w}$ the mean wind velocity, and w' the fluctuating wind velocity.

The wind-induced response and the total base shear of blades can be obtained by solving Eq.(1). With the theory presented by Nigam and Jennings (1968), the total base shear of the rotating blade can be equivalent to the inertia force summation of each point on the blade:

$$\boldsymbol{Q}_{\mathrm{B}}(t)=\sum_{i=1}^{n} m_i \ddot{\boldsymbol{v}}_i(t), \tag{3}$$

where $\boldsymbol{Q}_{\mathrm{B}}(t)$ is the absolute base shear of blade, m_i the mass of blade for element i, and $\ddot{\boldsymbol{v}}_i(t)$ the wind-induced acceleration at node i which can be obtained by Eq.(1).

The vibration equation of a tower under the wind loads can also be obtained by the D'Alembert principle and the dynamic FEM. To study the blade-tower coupling vibration, the effective shear is introduced into the vibration equation (Murtagh *et al*., 2005):

$$\boldsymbol{M}_{\mathrm{T}}\ddot{\boldsymbol{u}}+\boldsymbol{C}_{\mathrm{T}}\dot{\boldsymbol{u}}+\boldsymbol{K}_{\mathrm{T}}\boldsymbol{u}=\boldsymbol{F}_{\mathrm{T}}(t)+\bar{\boldsymbol{Q}}_{\mathrm{B}}(t), \tag{4}$$

where $\boldsymbol{M}_{\mathrm{T}}$ is the mass matrix of a tower, $\boldsymbol{C}_{\mathrm{T}}$ the damping matrix of the tower, $\boldsymbol{K}_{\mathrm{T}}$ the stiffness matrix of the tower, $\ddot{\boldsymbol{u}}$ the acceleration coordinates of the tower, $\dot{\boldsymbol{u}}$ the velocity coordinates of the tower, $\boldsymbol{u}$ the displacement coordinates of the tower, $\boldsymbol{F}_{\mathrm{T}}(t)$ the wind loads on the tower which can be calculated by Eq.(2), and $\bar{\boldsymbol{Q}}_{\mathrm{B}}(t)$ is the effective total base shear of blades.

With the blade-tower coupling effect, the effective shear of blades can be expressed as

$$\begin{aligned}\bar{\boldsymbol{Q}}_{\mathrm{B}}(t)=&[\ddot{\boldsymbol{v}}_1+\ddot{\boldsymbol{u}}_{\mathrm{top}}(t)]m_1+[\ddot{\boldsymbol{v}}_2+\ddot{\boldsymbol{u}}_{\mathrm{top}}(t)]m_2\\&+\cdots+[\ddot{\boldsymbol{v}}_n+\ddot{\boldsymbol{u}}_{\mathrm{top}}(t)]m_n,\end{aligned} \tag{5}$$

after substituting Eq.(3) into Eq.(5), $\bar{\boldsymbol{Q}}_{\mathrm{B}}(t)$ can be presented as

$$\bar{\boldsymbol{Q}}_{\mathrm{B}}(t)=\sum_{i=1}^{n} m_i\ddot{\boldsymbol{v}}_i(t)+\ddot{\boldsymbol{u}}_{\mathrm{top}}\sum_{i=1}^{n} m_i=\boldsymbol{Q}_{\mathrm{B}}(t)+\ddot{\boldsymbol{u}}_{\mathrm{top}}M_{\mathrm{B}}, \tag{6}$$

where M_{B} is the mass of the blades, and $\ddot{\boldsymbol{u}}_{\mathrm{top}}$ the acceleration coordinates at the top of the tower. The dynamic response of the tower under the total effective base shear of the blades and the wind loads along the tower can be solved by Eq.(4). The dynamic equilibrium equation of the tower can be solved by the Newmark method (Liu and Du, 2005).

NUMERICAL SIMULATIONS OF WIND VELOCITY TIME SERIES

Steady mean wind velocity

The wind-shear effect shows that the mean wind velocity is generally related to height and roughness length; by the index model, the mean velocity $V(h)$ can be expressed as

$$V(h)=V(h_0)(\lg(h/Z_0)/\lg(h_0/Z_0)), \tag{7}$$

where Z_0 is the roughness length, $V(h)$ the mean velocity at the height of h, and $V(h_0)$ the mean velocity at the height of h_0.

During the rotating process, the relationship between the height of each calculation point and the rotating speed of blades can be obtained:

$$h(t)=h_0+R\cos(\Omega t+\varphi), \tag{8}$$

where R is the rotating radius of the calculation point, h_0 the height of the hub, Ω the rotating speed of the blade, and φ the initial phase of the blade.

Fluctuating wind power spectrum and coherent coefficient

The fluctuating wind can be regarded as a 3D turbulent flow composed by the along-wind, across-wind and vertical-wind components. The capability characteristics of a fluctuating wind field can be described by its power spectrum in various directions. The along-wind dynamic response was considered only in this study, so the along-wind Kaimal fluctuating wind power spectrum was

$$\frac{fS(H,f)}{v_*^2}=\frac{200c}{(1+50c)^{5/3}}, \tag{9}$$

where f is the frequency of fluctuating wind, v_* the friction velocity, H the height of the simulation point, $c=fH/V(H)$ the dimensionless Monin coordinate, and $V(H)$ the mean wind velocity at the height of H.

A number of observations showed that the wind field had spatial coherence which should therefore be included in the simulation of fluctuating wind velocity on the wind turbine. Results of such site tests and wind tunnel tests show that spatial coherence related to space distance also decreases with the increase of space distance. Many types of coherent coefficient expressions were presented by the characteristics of spatial coherence. The Davenport coherent coefficient Coh_{ij} only including the vertical correlation can be expressed as (Li and Du, 2008)

$$Coh_{ij} = \exp\left(-\frac{fC_z(z_i - z_j)}{2\pi \times V(H)}\right), \tag{10}$$

where C_z is the vertical attenuation coefficient (we usually assume C_z=10), f the fluctuating wind frequency, and $V(H)$ the mean velocity at the height of H.

Harmony superposition method

The harmony superposition method is a discrete numerical method to simulate the steady random process (Shinozuka and Jan, 1972). The calculation points on the blades and tower have a vertical correlation, and the vertical correlation is only considered in this study. The fluctuating wind power spectrum including the vertical correlation can be obtained:

$$\boldsymbol{S}(\omega)_{n\times n} = \begin{bmatrix} S_{11} & & & & & \\ \vdots & \ddots & & & sym & \\ \vdots & \vdots & S_{ii} & S_{ij} & & \\ \vdots & \vdots & S_{ji} & S_{jj} & & \\ \vdots & \vdots & \vdots & \vdots & \ddots & \\ S_{n1} & \cdots & \cdots & \cdots & \cdots & S_{nn} \end{bmatrix}, \tag{11}$$

where S_{ii} is the auto-power spectrum of a fluctuating wind which is regarded as Eq.(9). S_{ij} is the cross-power spectrum which reflects the spatial coherence of fluctuating wind fields on the wind turbine, and can be expressed as

$$S_{ij}(\omega) = \sqrt{S_{ii}(\omega)S_{jj}(\omega)}Coh_{ij}, \tag{12}$$

where S_{ii} and S_{jj} are the auto-power spectrum of Points i and j, respectively (Kubota *et al*., 2008).

The fluctuating wind velocity time series can be regarded as a random process which is determined by its power spectrum. With the theory presented by Shinozuka (1971), the fluctuating wind velocity time series $\{w'(t)\}$ can be simulated as

$$w'(t) = \sqrt{2(\Delta\omega)}\sum_{m=1}^{M}\sum_{l=1}^{N}\left|\boldsymbol{H}_{jm}(\omega_{ml})\right|\cos(\omega_{ml}t - \theta_{jm}(\omega_{ml}) + \Phi_{ml}), \tag{13}$$

where N represents the division numbers of fluctuating wind frequency, and M refers to the calculation point numbers. $\Delta\omega=(\omega_u-\omega_0)/N$ indicates the frequency step, ω_u and ω_0 are the upper limit and lower limit circle frequencies of fluctuating wind, and Φ_{ml} denotes the uniformly distributed random numbers in [0, 2π]; $\boldsymbol{H}(\omega)$ is the Cholesky decomposition of power spectrum $\boldsymbol{S}(\omega)_{n\times n}$ as Eq.(14), and $\theta_{jm}(\omega)$ is the argument of $\boldsymbol{H}(\omega)$ as Eq.(15):

$$\boldsymbol{S}_{n\times n}(\omega) = \boldsymbol{H}_{n\times n}(\omega)\boldsymbol{H}^{\mathrm{T}}_{n\times n}(\omega), \tag{14}$$

$$\theta_{jm}(\omega) = \arctan\left\{\frac{\mathrm{Im}[\boldsymbol{H}_{jm}(\omega)]}{\mathrm{Re}[\boldsymbol{H}_{jm}(\omega)]}\right\}, \tag{15}$$

where $\boldsymbol{H}^{\mathrm{T}}(\omega)$ is the transposed matrix of $\boldsymbol{H}(\omega)$ (Note that its diagonal elements are real, but its off-diagonal elements are complex), and $\theta_{jm}(\omega)$ is the ratio of imaginary and real parts. To increase the period of the simulated sample, Shinozuka (1971) suggested that $\omega_{ml}=\Delta\omega(l-1)+\Delta\omega(m/M)$. The calculation spectrum approaches the target spectrum when N tends to become infinite.

NUMERICAL SIMULATION EXAMPLE

The structural model of a wind turbine consists of three rotating blades and an inverted cone type steel tower. The blades are made of GRP, and the rotating blades are simplified to cross-section rectangular cantilever beams (Fig.1). The length of each blade (L_B) is 30 m, the root width of the blade (L_R) is 3 m. The section sizes at the root and tip of each blade are illustrated as Section 1 and Section 2 in Fig.1. The rotating speed of each blade is taken as 2.856 rad/s, and the mass per unit length m is assumed to vary linearly form 150.38 kg/m at the base to 1.5038 kg/m at the tip. The axial elastic modulus is 6.25×10^{10} N/m^2, the radial elastic modulus is 1.65×10^{10} N/m^2, and the tangential elastic modulus is 0.55×10^{10} N/m^2. The Poisson ratio is 0.22, the structural damping ratio is 0.008, the aerodynamic damping ratio is 0.17, the drag coefficient of blade is taken as 2, and the air density is 1.25 kg/m^3. The height of tower is 80 m, and its section sizes at base and top are illustrated as Section 1 and Section 2 in Fig.2. The density of the tower is 7850 kg/m^3, the elastic modulus is 2×10^{11} N/m^2, the total mass of blades and hub is 19876 kg, the structural damping ratio is 0.01, the aerodynamic damping ratio is 0.09, the drag coefficient of tower is 1.2, the mean wind velocity at hub is taken as 25 m/s, and the roughness length is 0.1.

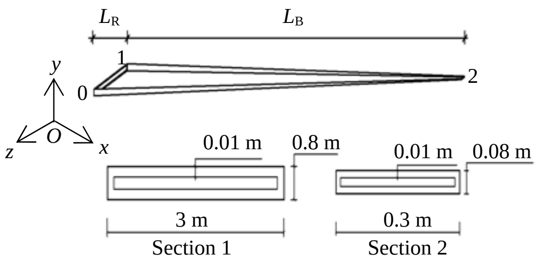

Fig.1 The cross-section rectangular cantilever beam model of blades

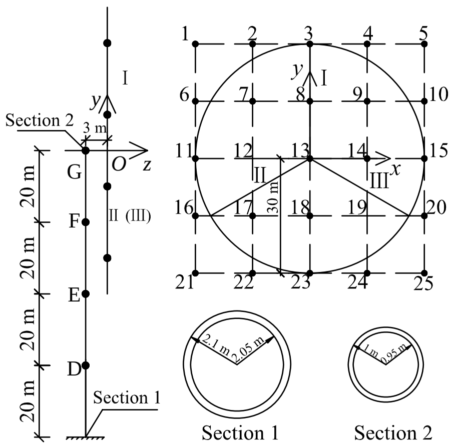

Fig.2 Calculation model of wind turbine and the fluctuating wind velocity calculation points

Numerical simulation of fluctuating wind velocity time series

The height (relative to the hub) of the calculation points on the blade are continuously changing during the rotating, so the mean wind velocity of each calculation point varies with the height. To carry out a real simulation of this situation, the relationship between mean wind velocity and rotating velocity can be obtained by the combination of Eqs.(7) and (8), and then the different mean wind velocities at different times of each calculation point on the rotating blade can be simulated. It is impossible to calculate each point's fluctuating wind velocities on the swept area, thus the swept area was divided into finite grids, and then the fluctuating wind velocities of these finite points can be calculated. The calculation results showed that the turbulent scale was between 5%~10% and the difference between each point was small, so the wind field of the swept area could be represented by these finite points. The fluctuating wind velocity could be calculated by the method presented in Section 2, and the position of each blade was illustrated as Fig.2. To obtain the fluctuating wind velocity time series of the blade and tower, 4 points on the tower and 25 points on the blade swept area were calculated. The calculation model was illustrated in Fig.2.

According to the above simulation method, the fluctuating wind velocity time series of the wind turbine were numerically simulated. Only the simulation results of Points G and 8 were illustrated in Fig.3 as the limited space.

Wind-induced responses of blade and tower

To analyze the wind-induced response of the tower, dynamic responses of the blade were analyzed first. The wind-induced response and the total base shear of blades can be obtained by Eqs.(1) and (2). The results of Blade I were only illustrated in Fig.4 as the limited space.

To analyze the influence of blade-tower coupling effects on the tower wind-induced response, the wind-induced response of the tower was calculated in time domain in two cases. One was the mass of the blades and the hub altogether being added at the top of the tower as a lumped mass, and the total base shear was excluded. The other was the included blade-tower coupling vibration, and the total effective base shear was introduced into the vibration equation of the tower. The wind-induced responses at the top of the tower in two cases were illustrated in Fig.5.

The wind-induced response calculation of blades is the foundation of investigating the blade-tower coupling effect. By the calculation results of Blade I, it can be seen that the maximum displacement at the tip of the blade is 0.826 m, and the maximum base shear is 55093.05 N. The calculation results of the blade show that the blade has large flexibility and its wind-induced responses are violent. The maximum displacement at the top of the tower is one of the most

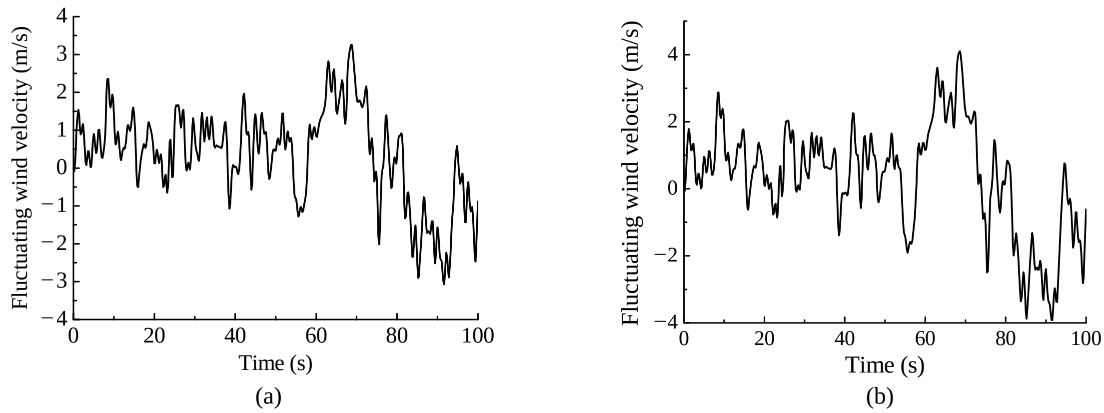

Fig.3 Simulated fluctuating wind velocity time series of (a) Point G and (b) Point 8

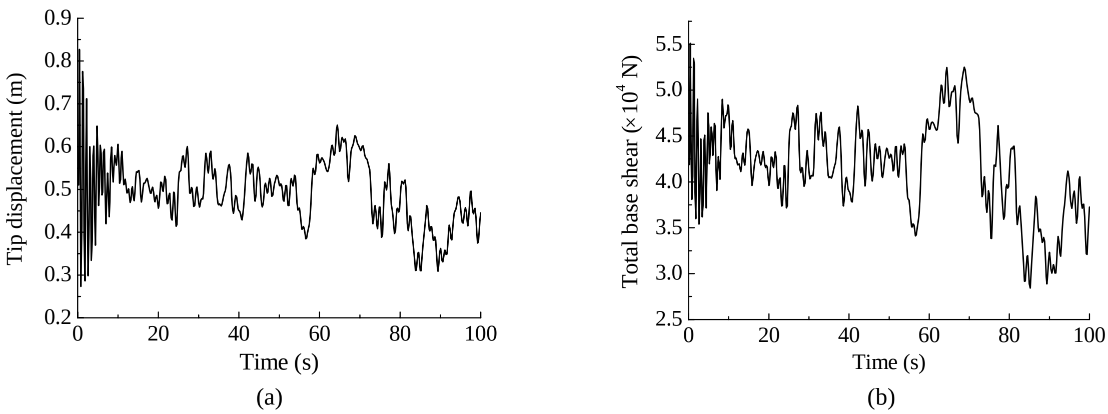

Fig.4 (a) Tip displacement response and (b) total base shear of Blade I

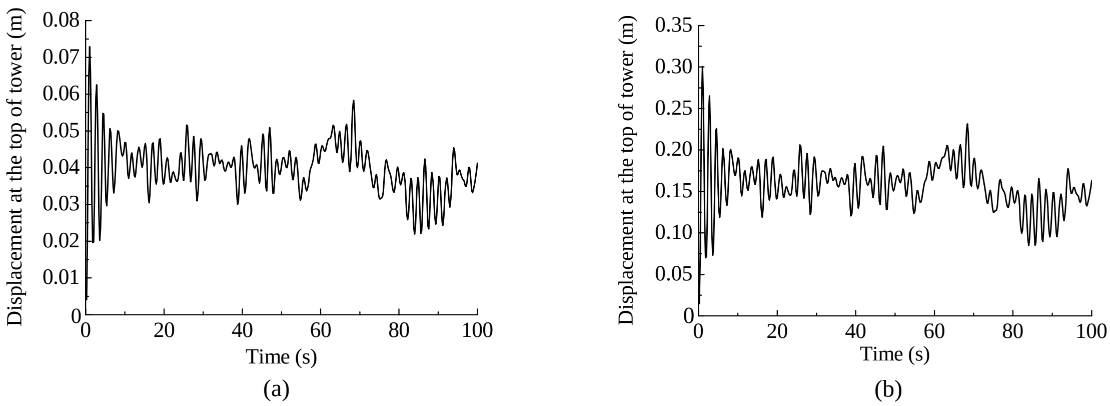

Fig.5 Wind-induced response at the top of tower in (a) Case 1 and (b) Case 2

important control indexes in the design of a wind turbine tower, so the maximum displacements of the two conditions were investigated. The maximum displacement at the top of the tower is 0.073 m in Case 1, and the maximum displacement at the top of tower is 0.291 m in Case 2. Comparing the maximum displacements of each case, the result of Case 2 increases nearly by 300% when the blade-tower coupling effect is included. The main reason of this difference is that the deformation of the blades and tower is large, and the components of this multi-body system have coupling effects during their vibration. Because of this deformation coupling between the components, the inertial force of the lumped mass needs to be added with the total base shear, and then the effective total base shear acting on the tower can be obtained. These effective base shears generate a great effect on the wind-induced response of the tower, especially the maximal displacement at the top of the tower. In the practical design of towers, the calculation method should include the blade-tower coupling effects, and then the reasonable and effective results could be obtained.

CONCLUSION

The wind-induced response of a wind tower was investigated, and the blade-tower coupling effect was also discussed in this paper. The blade had great flexibility, and its wind-induced responses were violent. Thus, the dynamic responses of the blade under wind loads exerted great influences on the wind-induced response of the tower. The approximate method for wind field simulation of rotating blades was presented, which could simulate the fluctuating wind velocity time series of rotating blades factually. When considering the vertical correlation of the calculation points and the outline of a wind turbine, the fluctuating wind velocity time series could be simulated by the power spectrum and the harmony superposition method. The wind-induced response at the top of the tower showed that the maximum displacement at the top of tower including the blade-tower effect increased nearly by 300% as compared to the case that the mass of the blade and hub was only added at the top of the tower. Obviously, the blade-tower coupling effect also has a significant impact on the maximum displacement at the top of the tower, and this deformation coupling can be calculated by the effective base shear of blades, thus it should be considered in the wind turbine design.

References

Baumgart, A., 2002. A mathematical model for wind turbine blades. *Journal of Sound and Vibration*, **251**(1):1-12. [doi:10.1006/jsvi.2001.3806]

Chattot, J.J., 2007. Helicoidal vortex model for wind turbine aero-elastic simulation. *Computers and Structures*, **85**(11-14):1072-1079. [doi:10.1016/j.compstruc.2006.11.013]

Clough, R.W., Penzien, J., 1975. Dynamics of Structures. Wang, G.Y., translators, 2006. Higher Education Press, Beijing, p.135-139 (in Chinese).

Deodatis, G., 1996. Simulation of ergodic multivariate stochastic process. *Journal of Engineering Mechanics, ASCE*, **122**(8):778-787. [doi:10.1061/(ASCE)0733-9399(1996)122:8(778)]

Di Paola, M., 1998. Digital simulation of wind field velocity. *Journal of Wind Engineering and Industrial Aerodynamics*, **23**(2):74-76.

Di Paola, M., Zingales, M., 2008. Stochastic differential calculus for wind-exposed structures with autoregressive continuous (ARC) filters. *Journal of Wind Engineering and Industrial Aerodynamics*, **96**(12):2403-2417. [doi:10.1016/j.jweia.2008.04.003]

Jelenic, G., Crisfield, M.A., 2001. Dynamic analysis of 3D beams with joints in presence of large rotations. *Computer Methods in Applied Mechanics and Engineering*, **190**(32-33):4195-4230. [doi:10.1016/S0045-7825(00)00344-3]

Jin, X., He, Y.L., Du, J., He, J., 2008. Coupled vibration analysis of wind turbine. *China Mechanical Engineering*, **19**(1):9-13 (in Chinese).

Kareem, A., 2008. Numerical simulation of wind effects: a probabilistic perspective. *Journal of Wind Engineering and Industrial Aerodynamics*, **96**(10-11):1472-1497. [doi:10.1016/j.jweia.2008.02.048]

Kubota, T., Miura, M., Tominaga, Y., Mochida, A., 2008. Wind tunnel tests on the relationship between building density and pedestrian-level wind velocity: Development of guidelines for realizing acceptable wind environment in residential neighborhoods. *Building and Environment*, **43**(10):1699-1708. [doi:10.1016/j.buildenv.2007.10.015]

Lanzafame, R., Messina, M., 2007. Fluid dynamic wind turbine design: critical analysis, optimization and application of BEM theory. *Renewable Energy*, **32**(14):2291-2305. [doi:10.1016/j.renene.2006.12.010]

Lavassas, I., Nikplaidis, G., Zervas, P., Efthimiou, E., Doudoumis, I.N., Baniotopoulos, C.C., 2003. Analysis and design of the prototype of a steel 1-MW wind turbine tower. *Engineering Structures*, **25**(8):1097-1106. [doi:10.1016/S0141-0296(03)00059-2]

Lee, C.L., Al-Salem, M.F., Woehrle, T.G., 2001. Natural frequency measurements for rotating span wise uniform cantilever beams. *Sound Vibration*, **240**(5):57-61.

Lesaffre, N., Sinou, J.J., Thouverez, F., 2007. Stability analysis of rotating beams rubbing on an elastic circular structure. *Journal of Sound and Vibration*, **299**(4-5):1005-1032. [doi:10.1016/j.jsv.2006.08.027]

Li, C.X., Du, M., 2008. Simulation of fluctuating wind velocity time series around super-tall buildings. *Journal of Vibration and Shock*, **27**(3):124-130 (in Chinese).

Liu, J.B., Du, X.L., 2005. Dynamics of Structure. China Machine Press, Beijing, p.139-147 (in Chinese).

Murtagh, P.J., Basu, B., Broderick, B.M., 2005. Along-wind response of a wind turbine tower with blade coupling subject to rotationally sampled wind loading. *Engineering Structures*, **27**(8):1209-1219. [doi:10.1016/j.engstruct.2005.03.004]

Naguleswaran, S., 1994. Lateral vibration of a centrifugally tensioned uniform Euler-Bernoulli beam. *Journal of Sound and Vibration*, **176**(5):613-624. [doi:10.1006/jsvi.1994.1402]

Nigam, N.C., Jennings, P.C., 1968. Digital Calculation of Response Spectra from Strong Motion Earthquake Records. Earthquake Engineering Research Laboratory Report, California Institute of Technology, USA.

Schindler, D., 2008. Responses of Scots pine trees to dynamic wind loading. *Agricultural and Forest Meteorology*, **148**(11):1733-1742. [doi:10.1016/j.agrformet.2008.06.003]

Shinozuka, M., 1971. Simulation of multivariate and multidimensional random process. *Journal of the Acoustical Society of America*, **49**(1B):357-367. [doi:10.1121/1.1912338]

Shinozuka, M., Jan, C.M., 1972. Digital simulation of random process and its application. *Journal of Sound and Vibration*, **25**(1):111-128. [doi:10.1016/0022-460X(72)90600-1]

Yang, J., 1972. Simulation of random envelope process. *Journal of Sound and Vibration*, **21**(1):73-85.

Yang, W.W., Chang, T.P., Chang, C.C., 1997. An efficient wind field simulation technique for bridge. *Journal of Wind Engineering and Industrial Aerodynamics*, **67-68**:697-708. [doi:10.1016/S0167-6105(97)00111-6]